

Development of an intelligent envelope system with energy recovery ventilation for passive dehumidification in summer and solar collection in winter

Yulu Chen^{1*}, Akihito Ozaki², Haksung Lee³, Younhee Choi², and Yusuke Arima²

¹Graduate School of Human-Environment Studies, Kyushu University, 744 Motoooka, Nishi-ku, Fukuoka 819-0395, Japan

²Faculty of Human-Environment Studies, Kyushu University, 744 Motoooka, Nishi-ku, Fukuoka 819-0395, Japan

³Department of Architecture, Chungbuk National University, 1 Chungdae-ro, Cheongju 28644, Republic of Korea

Abstract. With the aim of establishing a zero-energy housing (ZEH), an intelligent envelope system composed of a passive dehumidification and solar collection system (PDSC system) based on thermodynamic energy theory and an energy recovery ventilation (ERV) unit has been developed, abbreviated as PSE (PDSC & ERV) system, which can be expected to control the indoor hygrothermal environment by using renewable energy further to reduce the heating and cooling demand for the HVAC system. In this study, the measurement experiments were conducted in a wooden house equipped with a PSE system, and the temperature and humidity distributions in the rooms were assessed using thermo-hygrometer sensors. The field comparison experiments for the three systems (exhaust-only ventilation system, ERV system, and PSE system) were performed separately under various meteorological conditions in summer and winter. The measurement results in summer showed that the PSE system has a significant dehumidification effect compared to the exhaust-only and ERV-only ventilation systems and could effectively reduce the latent heat load caused by ventilation. The measurement results in winter indicated that the PSE system has the effect of heat collection and humidity control as well as reducing the sensible heat load originating from ventilation.

1 Introduction

The Japanese government declared a carbon-neutral goal in October 2020 to reduce greenhouse gas emissions to zero by 2050. This includes the requirement to ensure that housing and buildings meet the standards of Zero Energy houses (ZEHs) / Zero Energy Buildings (ZEBs) and the introduction of renewable energy sources. However, according to statistics, heating and cooling accounted for 27.5% of Japan's household sector energy consumption in 2020. Many studies on heat collection in winter or natural cooling in summer using renewable energy have been conducted to reduce the energy consumption of HVAC systems such as Trombe walls, solar air-heating systems, and cool roofs. Furthermore, it is well known that controlling indoor humidity levels is the most prominent means of reducing latent heat load, especially in hot and humid summer areas. Indoor humidity is an essential criterion for indoor hygrothermal comfort.

This study proposes an intelligent envelope system, which is a combination of a passive dehumidification and solar collection (PDSC) system and energy recovery ventilation (ERV), known as the PSE (PDSC combined with ERV) system. Difference from other existing air circulation systems, the PSE system is passive summer dehumidification and winter humidity control system

using solar energy, applying the theory of moisture transfer principle based on thermodynamic potential. The design of separating latent heat and sensible heat allows for good humidity control. Combining the heat- and moisture-recoverable ERV and the PDSC system makes it more efficient while ventilating to reduce the ventilation load, thereby reducing the demand for the indoor air conditioning system. Although our research group previously predicted excellent energy savings for the PSE system through numerical simulations, actual measurements are still needed to verify its effectiveness and practicality [1]. The experiments were conducted in a full-scale wooden house with a PSE system, and the temperature and humidity in the rooms were measured. The experimental results verified the superior summer dehumidification and winter heat collection characteristics of the PSE system over other systems (exhaust-only ventilation system and ERV).

2 Methodology

2.1 Moisture transfer principle of PDSC system

The moisture movement model in this study was obtained by applying the thermodynamic chemical potential to water diffusion, resulting in water potential (WP) as the driving force for water transfer (the detailed

* Yulu Chen: chen.yulu.062@s.kyushu-u.ac.jp

derivation process can be found in [2]). This approach is more accurate than other models based on physical properties (e.g., vapor pressure, absolute humidity, and water content) [3]. The WP can be represented by the thermodynamic energy and fundamental driving force of moisture transfer. The WP at a certain humid air status (known temperature and water vapor pressure) consists of its saturated and unsaturated WPs, and the relationship between them is shown in Figure 1. The following equations define these:

$$\mu_w(p, T) = \mu_w^0(T) + \mu(p, T) \quad (1)$$

$$\mu_w^0(T) = 6.44243 \times 10^5 + c_{p,w}(T - 273.15) - T c_{p,w} \ln \frac{T}{273.15} + R_w T \ln \frac{p_s}{1.01325 \times 10^5} \quad (2)$$

$$\mu(p, T) = R_w T \ln \frac{p_w}{p_s} \quad (3)$$

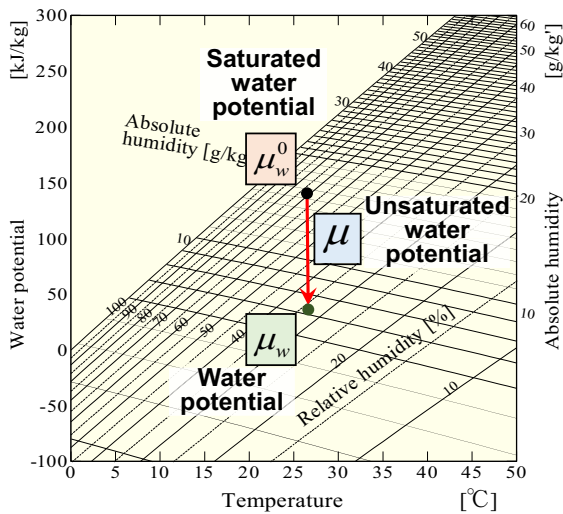


Fig. 1. Diagram of the relationship among water potential, temperature, relative humidity, and absolute humidity.

where μ_w is the WP in humid air at a certain dry-bulb temperature T and water vapor pressure p ; μ_w^0 and μ are expressed as its saturated WP and unsaturated WP, respectively; p_w and p_s are the vapor pressure and saturated vapor pressure of the humid air, respectively; and $c_{p,w}$ is the specific heat, which is expressed in $J/(kg K)$, and $R_w = 461.50 J/(kg K)$, which was calculated by dividing the gas constant R [$8.31441 J/(mol K)$] by the molecular weight of water ($18.01528 \times 10^{-3} kg/mol$).

The condition for reaching the thermodynamic equilibrium state is that each component's temperature, pressure, and chemical potential in a matter system is uniform; otherwise, matter spontaneously diffuses from the higher chemical potential to the lower chemical potential phase. WP is used as an indicator of the mass balance conditions in a system with a non-equilibrium state, where the moisture flux flows from the higher WP phase to the lower WP phase.

2.1.1 Summer mode

In summer, the WP difference between the indoor and roof ventilation layers was the driving force for moisture transfer during the daytime. Figure 2 shows a schematic diagram of the WP variations in the roof component during summer.

Assuming that the indoor temperature and humidity remain constant at 1 (DB (dry bulb temperature): 27 °C/ RH (relative humidity): 60%/ WP: 107.3 kJ/kg) in summer. During the day, the temperature of the roof increases with solar radiation, and the water vapor pressure of the porous hygroscopic material (insulation material that can absorb and release moisture in large quantities) in the roof increases; thus, moisture is desorbed into the ventilation layer, and the air state in the roof ventilation layer becomes 2 (DB:40 °C / RH:50%/ WP:160.2 kJ/kg). When the temperature of the roof ventilation layer reaches a particular condition,

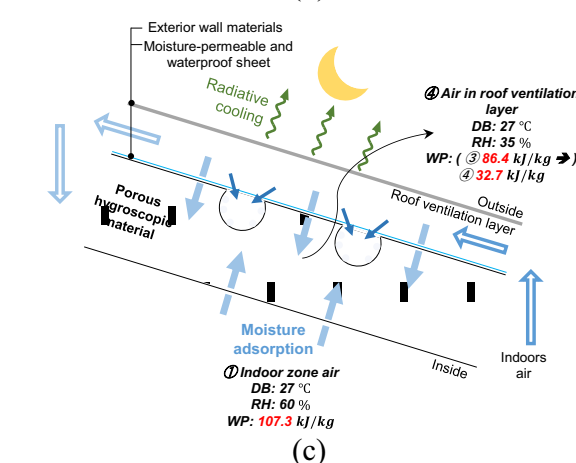
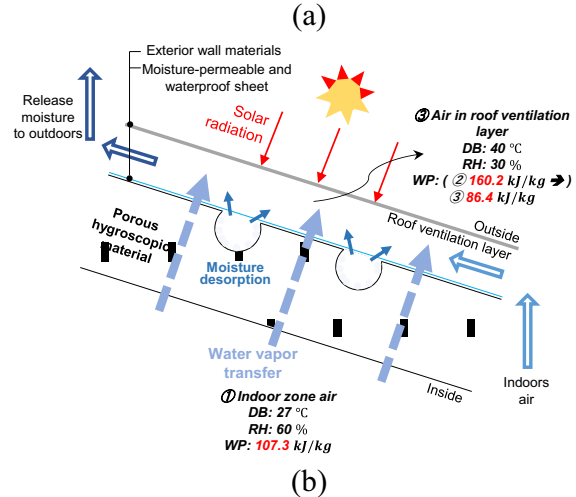
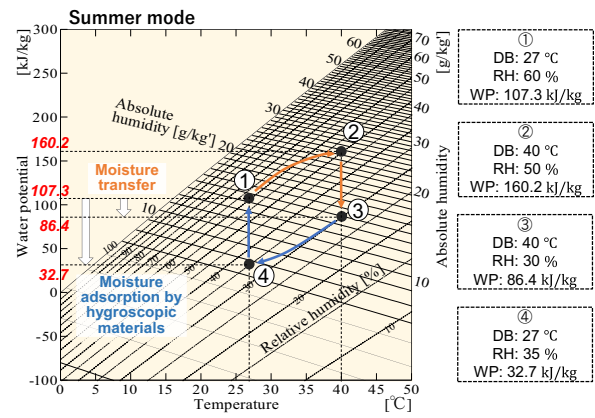


Fig. 2. PDSC system moisture movement diagram/Summer mode, (a) water potential, (b) moisture transfer during daytime and (c) moisture adsorption during night.

the indoor air is introduced into the ventilation layer by a low-power fan, and the absolute humidity in the ventilation layer drops to the same degree as that of the

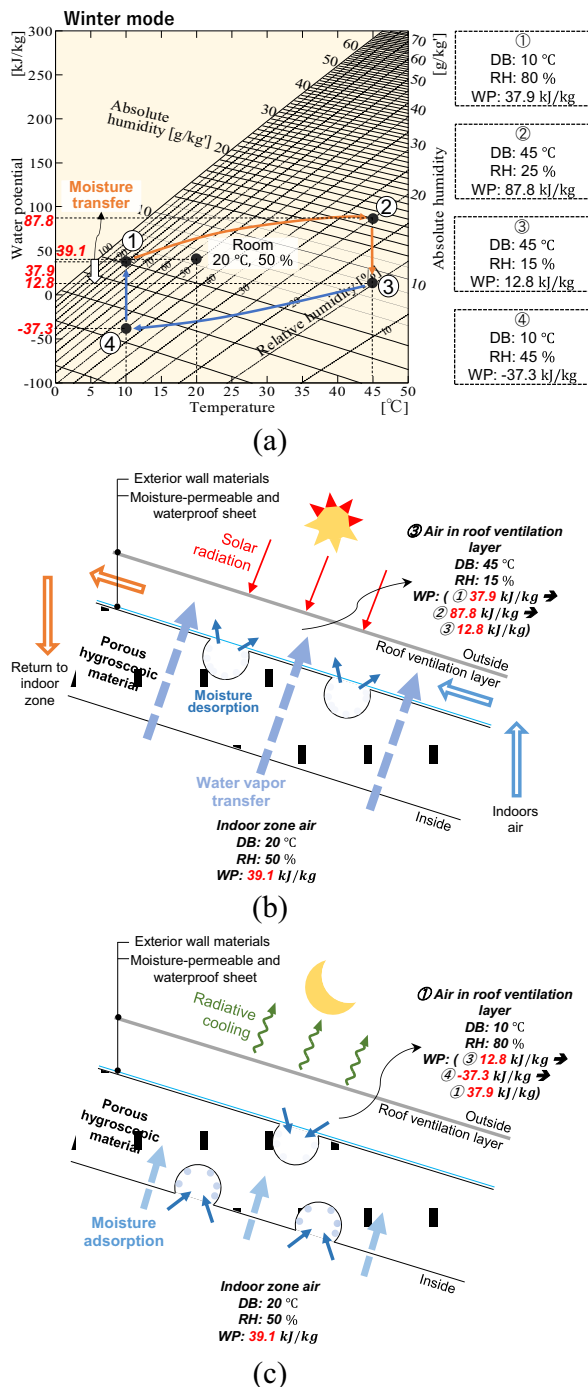


Fig. 3. PDSC system moisture movement diagram/Winter mode, (a) water potential, (b) Advection and moisture flow during daytime (c) moisture flow during night.

indoor air, resulting in the air status in the roof ventilation layer becoming 3 (DB:40 °C/ RH:30 %/ WP:86.4 kJ/kg). As a result, a WP difference is created between the indoor and the ventilation layer, and water flows from the indoor layer with high WP 1 to the ventilation layer with low WP 3, and is then released outdoors.

At night, the long wave radiation to the universe lowers the roof temperature, causing the porous hygroscopic material to adsorb moisture, and the status of the roof ventilation layer gradually changes to 4 (DB: 27 °C/ RH: 35 %/ WP: 32.7 kJ/kg). When the roof temperature meets a certain condition, indoor air is drawn into the ventilation layer and moisture is adsorbed

simultaneously. Then, the cooled and dried air is returned to the room. The WP in the roof gradually increases and reaches a final equilibrium indoors.

2.1.2 Winter mode: solar collection and humidity control

In winter, the indoor-roof air circulation only works during the day, and its WP difference follows the same pattern as that in summer. Figure 3 shows a schematic of the WP changes in the roof component during the winter.

It was assumed that the indoor temperature and humidity were maintained at 20 °C and 50%. During the day, the roof is heated by solar radiation, causing moisture to desorb from the porous hygroscopic material and diffuse to the roof ventilation layer, where the roof air state changes from 1 (DB:10 °C/ RH:80%/ WP:37.9 kJ/kg) to 2 (DB:45 °C/ RH:25%/ WP:87.8 kJ/kg). When indoor air is introduced into the ventilation layer, the status of the air inside the roof changes to 3 (DB: 45 °C/ RH:15%/ WP:12.8 kJ/kg). A WP difference is created, and moisture flows from the higher WP (room) to the lower WP 3 (roof ventilation layer). Therefore, the circulated air is heated and humidified in the roof ventilation layer, and eventually warm and humid air is distributed indoors.

At night, the temperature of the roof ventilation layer drops owing to the radiative cooling effect, causing the porous hygroscopic material to adsorb moisture, and the air in the roof becomes cooler and drier (low WP) 4 (DB:10 °C/ RH:45%/ WP: -37.3 kJ/kg).

2.2 Schematic diagrams of PSE system

The PSE system consisted of a roof-mounted PDSC system and an attic-mounted ERV. The ERV maintains a 0.5 ACH (air change per hour) ventilation rate with low energy loss, whereas the PDSC system regulates indoor temperature and humidity. The indoor air circulation pathway of the PSE system is divided into summer and winter modes.

2.2.1 Summer mode

Figure 4 shows the air circulation pathway of the PSE system during summer. During the daytime (Figure 4(a)), when the temperature inside the roof ventilation layer is higher than the indoor temperature plus 1 °C, indoor air is drawn into the roof ventilation layer by the exhaust air (EA) fan of the ERV. Moisture is transferred from the indoor environment to the roof ventilation layer. Then, the transferred moisture is directly discharged outdoors with the roof airflow without heat exchange, which completes dehumidification. Meanwhile, the ERV exchanges moisture and heat between the dehumidified indoor air and the hot and humid outdoor air while performing ventilation, maintaining low humidity indoors.

During the night (Figure 4(b)), when the temperature in the roof ventilation layer is lower than the indoor temperature minus 1 °C, the indoor air is introduced into

the roof ventilation layer by the ERV's supply air (SA) fan. The insulation material adsorbs moisture from the introduced indoor air. The dehumidified and radiatively cooled air is then transferred back to the room. Concomitantly, the ERV extracts moisture and heat from the outside air and transfers them to the RA stream to reduce the fresh air intake load.

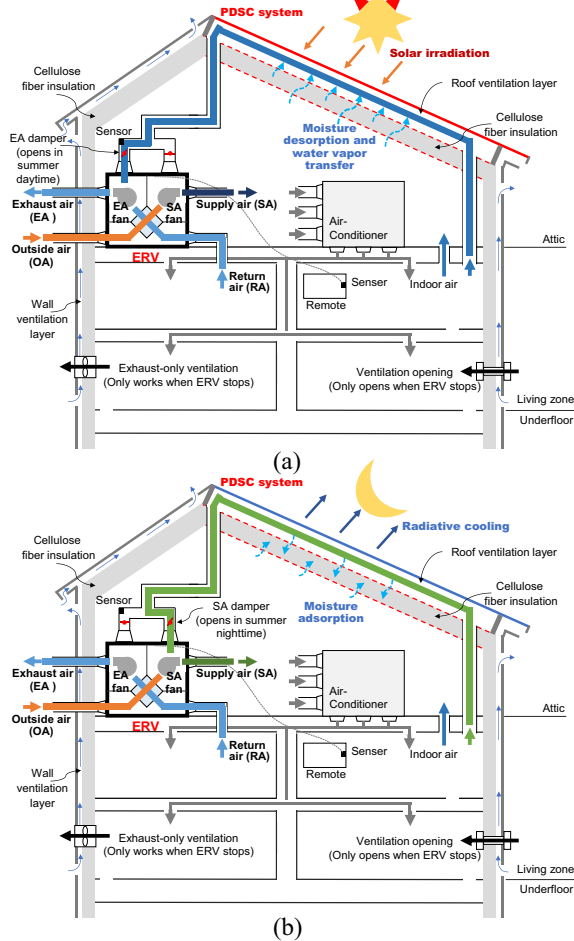


Fig. 4. Indoor-roof air circulation schematic of the PSE system in summer mode: (a) daytime and (b) night.

2.2.2 Winter mode

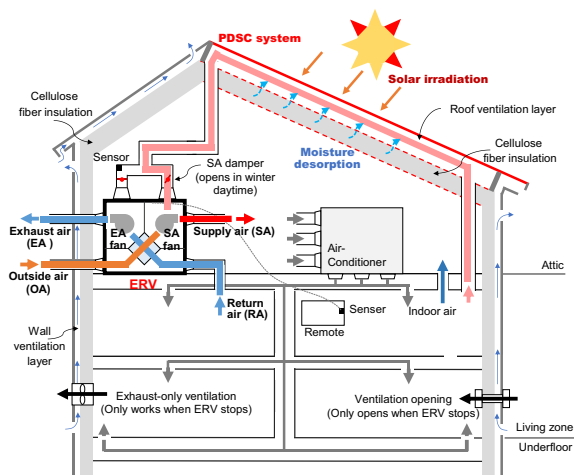


Fig. 5. Indoor-roof air circulation schematic of PSE system in winter mode

Figure 5 shows the air circulation pathway of the PSE system during winter. During the day, the temperature inside the roof increases because it receives solar radiation. As indoor air circulates into the roof ventilation layer (when the roof ventilation layer temperature is higher than the indoor temperature plus 1 °C), the air is heated inside the roof. Simultaneously, moisture is transferred from the indoor to the roof ventilation layer, and finally, warm and moist air is blown indoors. Therefore, the PSE system collects heat while suppressing the over-drying phenomenon caused by heating in winter. Concomitantly, heat and moisture are recovered from the RA to the outside air stream to reduce the heating load via the total heat exchanger.

2.3 Demonstration house equipped with PSE system

Table 1. Specifications of the demonstrated house.

Items	Description
Base ground (U-value 0.386 W/m ² K)	Inner to outer: phenolic foam insulation (thermal conductivity: 0.020 W/m K) t = 50 mm, concrete t = 160 mm
Walls (U-value 0.420 W/m ² K)	Inner to outer: interior finishing material, plaster board t = 12mm, cellulose fiber insulation t = 105 mm, structural plywood t = 9 mm, moisture-permeable and waterproof sheet, ventilation layer t = 18 mm, exterior finishing material
Floor	Top to bottom: Structural plywood t = 24 mm, flooring t = 12 mm
Ceiling	Top to bottom: Structural plywood t = 24 mm, flooring t = 12 mm
Roof (U-value 0.262 W/m ² K)	Inner to outer: cellulose fiber insulation t = 185 mm, moisture-permeable and waterproof sheet, roof ventilation layer t = 90 mm, structure plywood t = 12 mm, roofing, galvalume

A wooden house equipped with a PSE system was built in Yamaguchi Prefecture in Japan, where the summer weather is highly humid and hot and is relatively dry and cold in winter. Detailed building specifications are listed in Table 1. The photograph and floor plans are shown in Figure 6, where the dashed red line indicates the PDSC system. The construction of an ERV that provides power for indoor roof air circulation and ventilation is shown in Figure 7.

Cellulose fiber insulation (CFI) with high moisture capacity characteristics was installed in passive dehumidification systems (roofs) and building envelopes (walls). No waterproof sheet was attached to the interior side of the building enclosure to ensure that moisture could be adsorbed into (or desorbed out of) building materials. Room temperature and RH were monitored at 1-minute intervals using highly sensitive sensors with an accuracy of ±0.3 °C and ±5% RH (at 25 °C, 25% RH). Each room had a natural vent that opened when the ventilation fan in the lavatory performed exhaust-only ventilation.

2.4 Measurement condition

The measurements in this study explored the indoor temperature and humidity variations and ventilation heat loads of the PSE system compared with exhaust-only ventilation and ERV systems under different meteorological conditions in winter and summer, respectively.

The measurement conditions are listed in Table 2. The experiments were roughly divided into Case A (summer mode) and Case B (winter mode), each with six scenarios. Cases 1, 2, and 3 were in a non-air conditioned state, and Cases 4, 5, and 6 were in an air-conditioned state (cooling: 27°C/heating: 20°C). Notably, no heat and moisture generation by humans indoors. During the summer daytime, the ventilation rate through the roof (then exhausted outdoors) was 70 m³/h, and the ERV exhaust rate was 100 m³/h (for a total ventilation rate of 170 m³/h ≈ 0.5 ACH). At night, the airflow rate inside the roof (then returned indoors) was 170 m³/h, and the ventilation rate of the ERV was 170 m³/h (≈0.5

ACH). The air circulation pattern during winter daytime was the same as that during summer night.

The corresponding calculation procedure of the ventilation latent heat load in summer and sensible heat load in winter under air conditioning can be described as follows: (1) Latent heat load by ventilation in summer, which can be calculated based on the ventilation rate and absolute humidity difference between the indoor and outdoor air for Case A-4 (exhaust-only ventilation system). Case A-5 (ERV system) used the absolute humidity difference between the return and SA and the ventilation rate of the ERV, and Case A-6 (PSE system) was calculated by subtracting the dehumidification capacity of the PDSC system (calculated based on the airflow rate and absolute humidity difference between the inlet and outlet of the roof ventilation layer) from the same calculation equation as in Case A-5. (2) Sensible heat load by ventilation in winter in which the calculations are similar to the latent heat, where the temperature difference replaced the humidity difference.

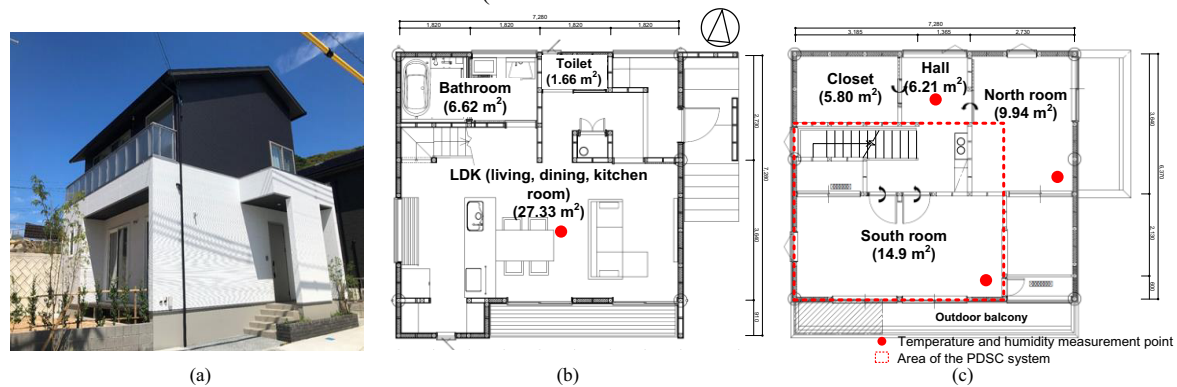


Fig. 6. Demonstrated house (a) Exterior appearance, (b) first floor plan, and (c) second floor plan.

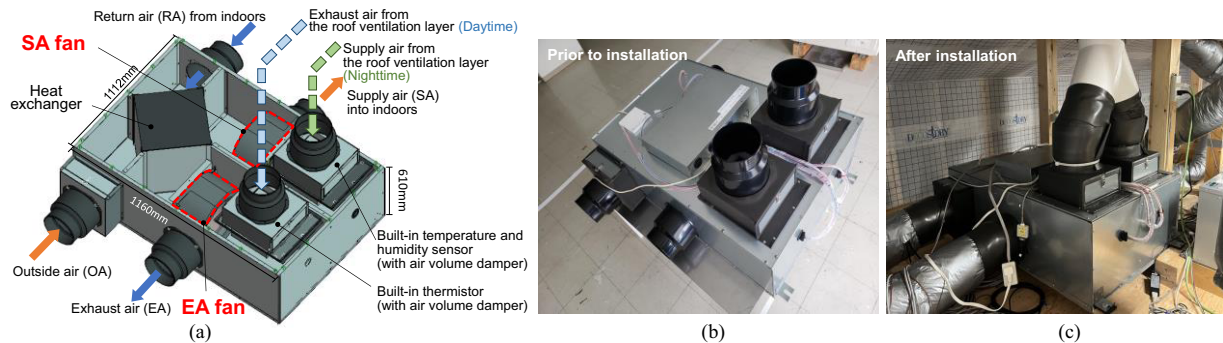


Fig. 7. ERV unit (a) ERV composition and (b) photograph prior to installation and (c) photograph after installation.

Table 2. Measurement conditions in summer and winter.

Modes	Cases	AC (Air conditioner)	Ventilation systems	PDSC system operation condition
A: Summer mode	A-1	AC off (May 18, 2022 – Jun. 22, 2022)	Exhaust-only ventilation	Daytime: ON: $T_{roof} > T_{room} + 1\text{ }^{\circ}\text{C}$ OFF: $T_{roof} < T_{room}$ Nighttime: ON: $T_{roof} < T_{room} - 1\text{ }^{\circ}\text{C}$ OFF: $T_{roof} > T_{room}$
	A-2		ERV	
	A-3		PSE (PDSC + ERV)	
	A-4	AC on: Cooling 27°C (Jun. 24, 2022 – Aug. 09, 2022)	Exhaust-only ventilation	
	A-5		ERV	
	A-6		PSE (PDSC + ERV)	
B: Winter mode	B-1	AC off (Nov. 09, 2021 - Dec. 27, 2021)	Exhaust-only ventilation	Daytime: ON: $T_{roof} > T_{room} + 1\text{ }^{\circ}\text{C}$ OFF: $T_{roof} < T_{room}$
	B-2		ERV	
	B-3		PSE (PDSC + ERV)	
	B-4	AC on: Heating 20 °C (Dec. 29, 2021 – Feb. 24, 2022)	Exhaust-only ventilation	
	B-5		ERV	
	B-6		PSE (PDSC + ERV)	

3 Results

3.1 Results without air-conditioning

3.1.1 Summer mode

Figure 8 illustrates the intercepted 3-day measured temperature and humidity values of the exhaust-only ventilation, ERV, and PSE system in summer (2022 year) without air conditioning. Because the envelope of the experimental house is equipped with ventilation layers, and the CFI inside the walls can perform extensive moisture adsorption and desorption, the indoor RH of the exhaust ventilation system (Case A-1) was relatively stable (Figure 8(d)). Additionally, the average absolute humidity difference between LDK and outdoor air is approximately 0.27 g/kg (DA). Notably, the exhaust ventilation system directly draws humid outdoor air into the room. However, when ERV was operated (Case A-2), the average absolute humidity difference between LDK and outside air was approximately 0.87 g/kg (DA). When PDSC and ERV were combined (Case A-3), the PDSC system excluded moisture transferred to the outside during the day, resulting in an absolute humidity at the roof outlet as high as 19.9 g/kg (DA) (Figure 8(i)). At night, the SA included air adsorbed in the roof and dehumidified by the ERV so that the average absolute humidity difference between the LDK and outside air increased to 2.0 g/kg (DA), which was significantly higher than that in Cases A-1 and A-2. Moreover, the indoor RH of Case A-3 was relatively stable, showing an almost straight line and remaining below 58%.

Figure 9 shows the distribution and cumulative rate of the whole observation period absolute humidity data

in summer without air-conditioning. It can be seen that the absolute humidity inside is slightly lower than outside due to the moisture adsorption and desorption characteristics of the building envelope in the exhaust-only ventilation system (Case A-1). When ERV was worked (Case A-2), the ERV could recover moisture from incoming outdoor air and transfer it to the exhaust air due to the absolute humidity difference between indoor and outdoor. The larger the absolute humidity difference between indoors and outdoors, the more moisture the ERV can transfer. The distance between the indoor and outdoor absolute humidity curves of the

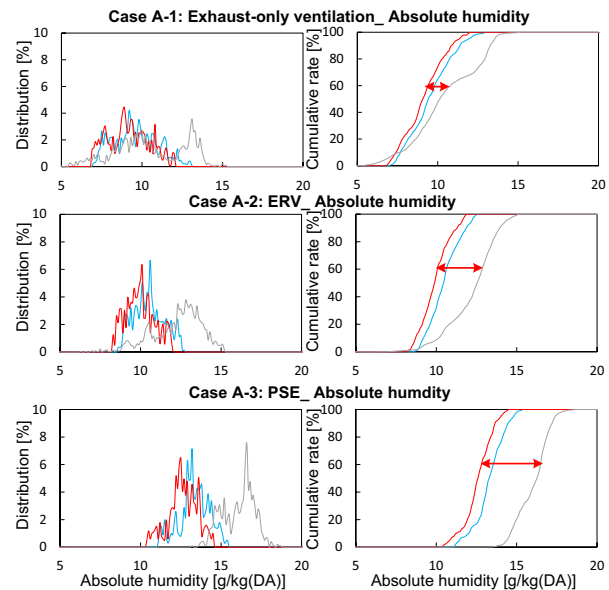


Fig. 9. Distribution and time cumulative rate of relative and absolute humidity in main rooms without air-conditioning.

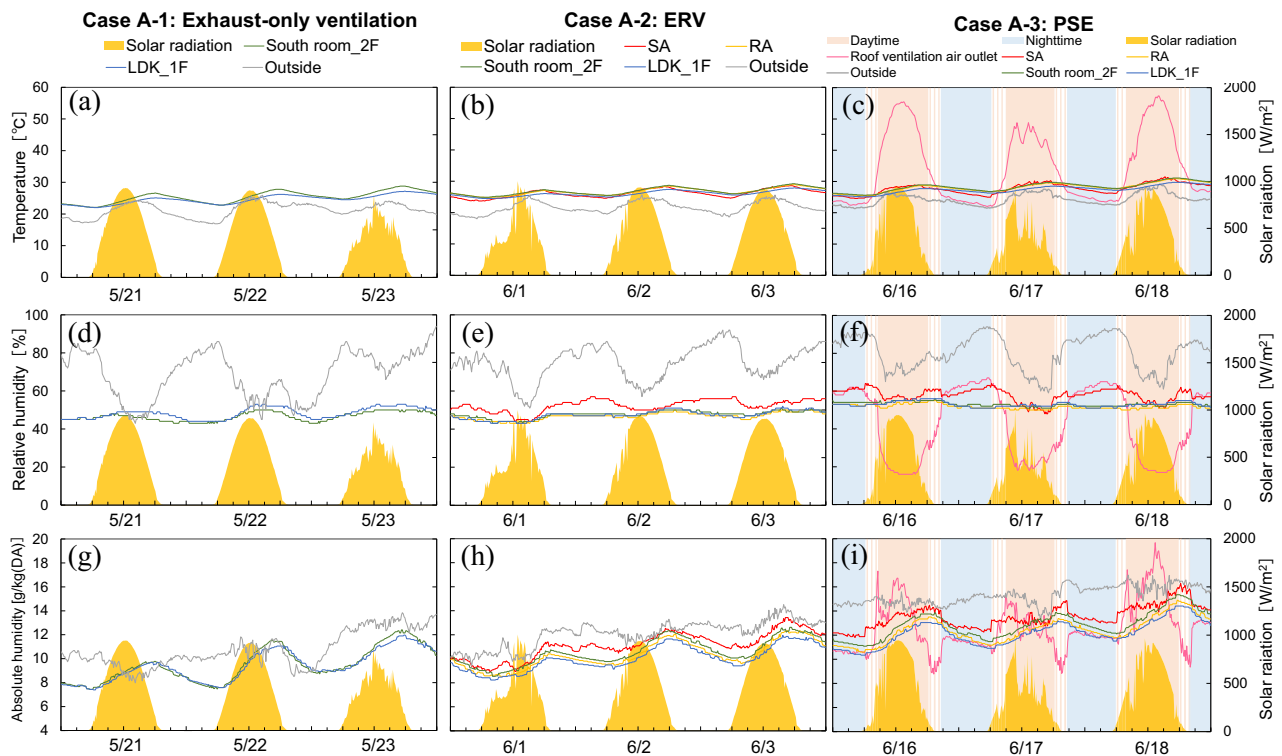


Fig. 8. Comparison of the temperature and humidity for the main room in summer without air-conditioning.

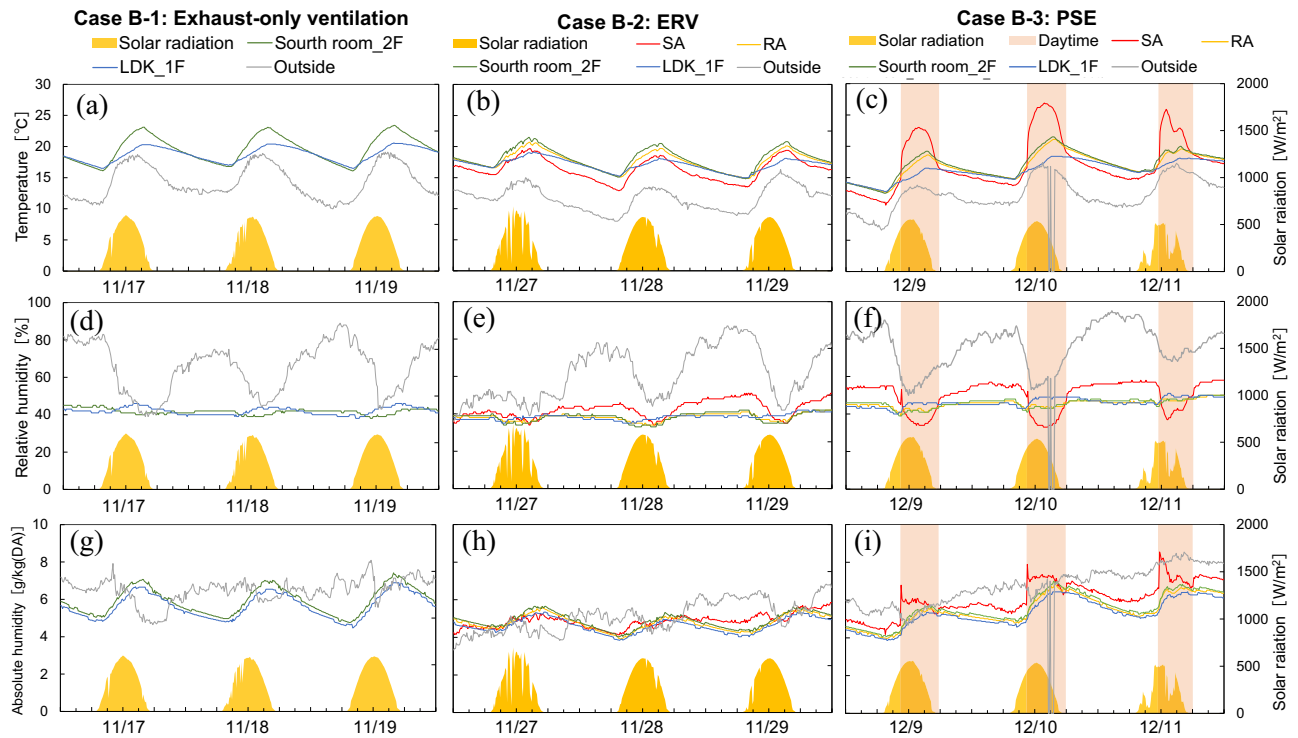


Fig. 10. Comparison of the temperature and humidity for the main room by using various system in winter without air-conditioning.

PSE system was the farthest, indicating that PSE had a remarkable dehumidification effect compared to exhaust- and ERV-only systems in hot and humid summers without air conditioning.

3.1.2 Winter mode

Figure 10 illustrates the intercepted 3-day measured temperature and humidity values of the exhaust-only ventilation, ERV, and PSE system in winter (2021) without air conditioning. In the case of maintaining a constant ventilation rate, ERV, while conducting ventilation different from the exhaust-only ventilation system, could recover heat from the RA and transmit it to the SA. Therefore, the SA temperature in the ERV system (Case B-2) was much higher than that of the outside air, and the average daily temperature difference between SA and outside air was 4.6 °C. In the case of the SC system (because there is no passive dehumidification in winter, it is called the SC system), the combined heated air from the roof and the warm SA from the ERV were returned to the room during the day. Thus, the daily average temperature difference between SA and indoor air increased to 4.9 °C, and the difference in instantaneous values could be up to 10 °C, confirming the excellent heat collection performance of the SC system in winter. In addition, the SA absolute humidity of the SC system was significantly higher than that of the indoor air during the daytime because the moisture transferred from the roof was returned to the room with the airflow. Thus, the SC system could maintain indoor relative humidity stability in a heated environment, which alleviates room air from over-drying due to heating.

3.2 Results with air-conditioning

3.2.1 Summer mode

- Case A-4: Exhaust only ventilation_ AC cooling: 27°C
- Case A-5: ERV_ AC cooling: 27°C
- Case A-6: PSE_ AC cooling: 27°C

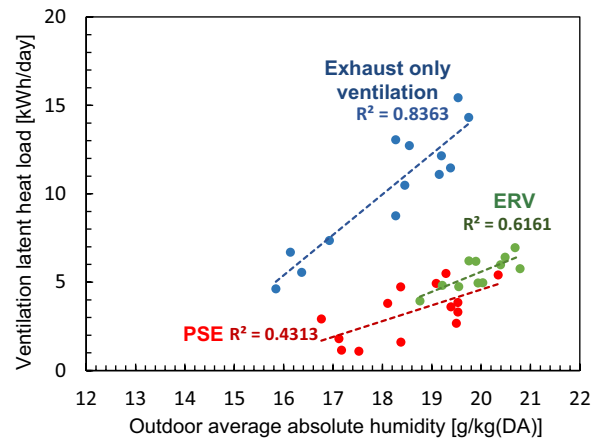


Fig. 11. Comparison of the ventilation latent heat load in summer with air-conditioning

Figure 11 shows the ventilation latent heat load in the summer with air conditioning (cooling: 27 °C). The x-axis corresponds to the daily outdoor average absolute humidity and the y-axis corresponds to the daily ventilation latent heat load. As the average absolute outdoor humidity increased, the latent heat load of the ventilation system increased as the amount of water vapor entering the room increased. The ventilation latent heat load of the ERV system decreased significantly for the same average absolute outdoor humidity because the ERV dehumidified the high-humidity outside air when it was ventilated. In the PSE system, the PDSC system dehumidified the indoor environment, and the difference between indoor and outdoor humidity was significant; thus, the moisture recovered by the ERV

increased owing to the increase in the humidity difference between the return and outdoor air. Therefore, the PSE system had the lowest ventilation latent heat load compared with the exhaust-only ventilation and ERV systems under similar outdoor average absolute humidity.

3.2.2 Winter mode

Figure 12 shows the ventilation sensible heat load in winter with air-conditioning (heating at 20°C). The x-axis corresponds to the daily outdoor average temperature and the y-axis corresponds to the daily ventilation sensible heat load. The sensible heat load graph shows the same trend as that in summer. For similar outdoor average temperatures, the exhaust-only ventilation system showed the highest sensible heat load, followed by the ERV and PSE systems. This is because when the ERV works, it recovers heat from the warm inside RA to the fresh and cold outside SA; thus, the air conditioner has lower heating costs to deal with in the presence of the ERV. If the heat collection effect from the SC system is added with ERV, the heat load is further reduced, and it is possible to make the total sensible heat load of the PSE system equal to or less than zero.

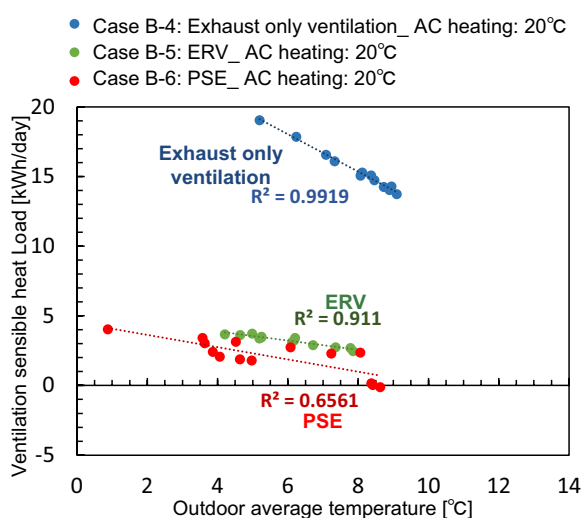


Fig. 12. Comparison of the ventilation sensible heat load in winter with air-conditioning

4 Conclusions

This study proposes an efficient hygrothermal-regulated PSE system that combines an ERV and an intelligent summer passive dehumidification and winter heat collection envelope system. The practicality and efficiency of the PSE system were verified through field experiments. Comparison experiments of the PSE system and other ventilation systems were conducted in summer and winter, respectively. The experimental results are as follows: In non-air conditioning status of summer, the PSE system could maintain a stable indoor RH of less than 58%, and the absolute humidity difference between indoor and outdoor is up to 2.0 g/kg (DA), which is significantly higher than that of the exhaust-only and ERV-only systems. In non-air

conditioning status of winter, the PSE system can demonstrate an excellent heat collection effect during the daytime and alleviate the disadvantage of excessive dryness during heating. In the air-conditioning status of summer, the ventilation latent heat load of the PSE system was the lowest under the same outdoor average absolute humidity condition. In the air-conditioning status during winter, the ventilation sensible heat load of the PSE system is the lowest under the same outdoor average temperature conditions. Furthermore, in times of high daily radiation, the ventilation sensible heat load can be equal to or even less than zero, indicating that the heat collection of the SC system is greater than the heat lost by ventilation. In conclusion, the PDSC system and ERV combination have excellent passive dehumidification in summer and heat collection and humidity regulation performance in winter, and can reduce the sensible and latent heat load of the air-conditioning system.

However, this study conducted experiments on the PSE and other systems under different meteorological conditions. Numerical analysis is necessary to understand the performance of the PSE system in greater detail. High-precision simulation software will be used to reproduce the distribution of indoor temperature and humidity environments in future research and explore the temperature and humidity regulation and energy-saving effects of the PSE system compared with other ventilation systems under the same meteorological conditions.

This work was supported by JST, the establishment of university fellowships for the creation of science and technology innovation (Grant Number JPMJFS2132). This work was supported by the National Research Foundation of Korea (NRF) grant funded by the Korea government (MSIT) (No. RS-2023-00210812).

References

- [1] Y. Chen, A. Ozaki, H. Lee, Energy saving potential of passive dehumidification system combined with energy recovery ventilation using renewable energy, *Energy Build.* 268 (2022) 112170. <https://doi.org/10.1016/j.enbuild.2022.112170>.
- [2] A. Ozaki, T. Watanabe, T. Hayashi, Y. Ryu, Systematic analysis on combined heat and water transfer through porous materials based on thermodynamic energy, *Energy Build.* 33 (2001) 341–350. [https://doi.org/10.1016/S0378-7788\(00\)00116-X](https://doi.org/10.1016/S0378-7788(00)00116-X).
- [3] Y. Choi, W. Cho, A. Ozaki, H. Lee, Influence of the moisture driving force of moisture adsorption and desorption on indoor hygrothermal environment and building thermal load, *Energy Build.* 253 (2021) 111501. <https://doi.org/10.1016/j.enbuild.2021.111501>.